ASIAN JOURNAL OF PHARMACEUTICAL AND CLINICAL RESEARCH

INNOVARE ACADEMIC SCIENCES
Knowledge to Innovation

Vol 19, Issue 3, 2026

Online - 2455-3891
Print - 0974-2441

Research Article

GREEN SYNTHESIS OF IRON OXIDE NANOPARTICLES FROM *PLECTRANTHUS AMBOINICUS* AND THEIR WIDE RANGE OF BIOMEDICAL APPLICATIONS

YATAKONA SUPRIYA, SATHASIVAM SIVAMALAR*

Department of Research, Meenakshi Academy of Higher Education and Research, Chennai, Tamil Nadu, India.
***Corresponding author: Dr. Sathasivam Sivamalar; Email: sv.biotech@gmail.com**

Received: 11 November 2025, Revised and Accepted: 24 January 2026

ABSTRACT

Objective: Green synthesis of metal nanoparticles provides an environmentally friendly approach in comparison with the chemical method. Iron oxide nanoparticles (FeONPs) have potential biomedical applications such as antimicrobial, antioxidant, and anti-inflammatory activities. The goal of the current study was to synthesize FeONPs using the leaf extract of *Plectranthus amboinicus* and to assess the biological activities.

Methods: FeONPs were prepared in a green reduction and stabilization method using aqueous extracts of *P. amboinicus* leaves. The formation of FeONPs was initially qualitatively identified through colorimetry and additionally identified using ultraviolet (UV)-visible spectroscopy, X-ray diffraction (XRD), and Fourier transform infrared spectroscopy (FTIR). Antimicrobial testing was conducted against *Staphylococcus aureus*, *Staphylococcus epidermidis*, *Streptococcus mutans*, *Aggregatibacter actinomycetemcomitans*, and *Candida albicans* using minimum inhibitory concentrations (MIC) and time-kill methods. The antioxidant property of the synthesized FeONPs was evaluated using the 2,2-diphenyl-1-picrylhydrazyl radical scavenging assay. The anti-inflammatory property was analyzed by protein denaturation inhibition assays utilizing bovine serum albumin and egg albumin models. The cytotoxicity as well as the toxic properties of FeONPs were analyzed by brine shrimp (*Artemia salina*) lethality bioassays.

Results: The emergence of a clear color transition from dark brown to light brownish-orange signified nanoparticle development, accompanied by a distinctive UV–Visible Spectroscopy absorption wavelength at 395 nm. XRD pattern verification demonstrated the nanocrystalline and phase-pure quality of FeONPs, measuring 10–12 nm. FTIR pattern matching further demonstrated surface modification by OH, aromatic, and phenolic moieties. The MIC range was 25–100 µg/mL, demonstrating broad-spectrum antibacterial activity, considerable antioxidant activity, and moderate anti-inflammatory activity. Cytotoxicity studies also exhibited moderate cell toxicity with LC_{50} = 8 µg/mL.

Conclusion: Green-synthesized FeONPs using *P. amboinicus* demonstrated stability, multifunctional bioactivity, and promising antimicrobial, antioxidant, and anti-inflammatory properties, highlighting their potential for further *in vivo* biomedical applications.

Keywords: Green synthesis, Iron oxide nanoparticles, *Plectranthus amboinicus*, Antimicrobial activity, Antioxidant activity, Cytotoxicity, Biomedical applications.

 DOI: http://dx.doi.org/10.22159/ajpcr.2026v19i3.57457. Journal homepage: https://innovareacademics.in/journals/index.php/ajpcr

INTRODUCTION

The advent of nanotechnology in research has allowed scientists to work with matter on an atomic/molecular scale. Of these nanomaterials, iron oxide nanoparticles (FeONPs) have received increasing attention because of their outstanding physicochemical properties such as high surface-to-volume ratio, magnetism, conductivity, and catalytic capability [1,2]. Due to these capabilities, FeONPs have immense potential in different medical realms such as carrying drugs, imaging, sensing, and antimicrobial treatment. In general, conventional methods in physics and chemistry used in producing such nanomaterials require higher energy input and toxic reagents, which pose serious ecological toxicity [3]. Biological methods in synthesizing these nanomaterials have thus become not only non-hazardous and less expensive but also a very environmentally sound and cost-effective technology in this front [4,5].

Green nanotechnology focuses on using biological materials such as plant extracts, microorganisms, and biopolymer mediators to produce nanoparticles with minimal usage of toxic chemicals or in complete avoidance of them [6]. Among these, phytochemical methods have proven to be important because they are simple, can be easily scaled up, and have a wide variety of available plant materials which can work as natural reducing agents [7]. During reduction reactions between metal ions, such as ferric ions in ferric chloride, and phytochemicals such as flavonoids, terpenoids, and other water-soluble compounds, nanoparticles are produced and simultaneously stabilized [8].

Having a long history of rich herbal traditions, coming down from the Rigveda, makes India a treasure trove of herbs that possess enormous potential for applications in green nanotechnology. The scientific categorization of herbs according to their therapeutic potential in ayurvedic practices provides a scientific and useful platform for exploiting their biological potential for nanotechnology applications [9]. Among these herbs, *Plectranthus amboinicus* emerges as a highly valuable and much-unutilized aromatic herb with immense therapeutic potential. Being a traditionally proven herb in ancient systems of medicine, it still finds useful applications for its efficacy in curing respiratory, gastrointestinal, and dermatological disorders [10]. The herb is rich in biologically valuable active phytoconstituents, including active volatile oils that account for its diverse, broad-spectrum pharmaceutical, and therapeutic potential. In addition, the diverse geographical variations in phytoconstituents of *P. amboinicus*, primarily due to climatic and edaphic conditions of cultivation, emphasize region-wise evaluations of their biological contents for making a complete utility of its valuable applications in nanotechnology [11].

Although green synthesis methods using plant extracts have been widely studied in the synthesis of nanoparticles, most studies employing *P. amboinicus* have dealt with the synthesis of silver, gold, zinc oxide, and other metal nanoparticles. However, in the synthesis of FeONPs using the extracts of plants, very few studies have been documented to date, in which *P. amboinicus* can remain an unexplored

area. Therefore, it can be concluded that this study not only provides an innovative avenue in using *P. amboinicus* in the green synthesis of FeONPs based on the rich range of phytochemicals present in this herb to improve the stability, biocompatibility, and medicinal properties of FeONPs but will also help in developing eco-friendly biologically active FeONPs in the field of nanobiotechnology.

Due to the overuse of antibiotics, antimicrobial resistance is growing, and hence, plant-based antimicrobials have gained high importance. *P. amboinicus* has been regarded as a highly potent antimicrobial plant that has great potential in using it for nanoparticle-based medical, anticancer [12], and antimicrobial functions. In this manuscript, *P. amboinicus* leaves extract will be used for the production of FeONPs by following an eco-friendly and green technique. Further, the derived nanoparticles will be used to analyze their characterization and antimicrobial activities. In this regard, the study will focus on enhancing green nanotechnology to fabricate a much safer, cost-effective, and environmentally sound method for the preparation of biologically active nanoparticles.

METHODS

Leaves of *P. ambonicus* were collected during August from Annaji Nagar, Chennai, Tamil Nadu. The bacteria include *Staphylococcus aureus* [29213], *Staphylococcus epidermidis* [14990], *Streptococcus mutans* [25175], *Candida albicans* [10231], and *Aggregatibacter actinomycetemcomitans* [29522], which were provided from the American Type Culture Collection (ATCC). Ferric chloride ($FeCl_3$), CAS No.: 7705-08-0, purchased from Merck, India. Mueller-Hinton Agar was obtained from HiMedia, Mumbai. All experimental processes with microbial cultures were carried out under aseptic conditions in biosafety cabinet class A2 as per institutional biosafety protocols to reduce the chances of contamination and to facilitate safe handling of pathogenic microbes.

Preparation of aqueous extract

A total of 5 g of fresh *P. amboinicus* leaves were obtained. The impurities were washed away from the leaves 3–4 times using double-distilled water and kept for dry on tissue paper, and their net weight after purification was noted for reproducibility. The purified leaves were cut into small pieces and dried at room temperature (25–28°C) for 3–5 days to a constant weight. The dried sample was finely powdered using a mortar and pestle, and 50 mL of double-distilled water was subsequently added [13]. The sample was heated in hot-water extraction for 30 min at 56°C with occasional stirring. The resulting extract was filtered through Whatman No. 1 filter paper and preserved at 4°C for future use. While solvent extraction is frequently employed to recover a wider range of secondary metabolites, aqueous hot-water extraction was specifically chosen to facilitate a green and biocompatible process amenable to downstream nanoparticle synthesis, and this constraint has been recognized as a factor for future work.

Iron nanoparticle synthesis

The mixture was prepared by adding 20 mM ferric chloride ($FeCl_3$) to 70 mL of deionized water, followed by the addition of 30 mL of filtered *P. amboinicus* extract. The reaction mixture was magnetically stirred at a speed of 600–700 rpm for a period of 48 h. The pH of the reaction mixture was reduced to pH 8.0, since higher alkaline conditions favor the stability of FeONP. The reaction mixture was centrifuged at a speed of 8000 rpm for a period of 10 min; the pellets obtained were further cleaned with ethanol and deionized water 3 times and then dried at a temperature of 70°C for a period of 2 h. The obtained dried FeONPs are then packed in airtight Eppendorf tubes for further analysis [14,15] (Fig. 1).

Characterization

The characterization of FeONPs synthesized was carried out by the application of characterization techniques such as ultraviolet (UV)-visible spectroscopy, X-ray diffraction (XRD), and Fourier transform infrared spectroscopy (FTIR) analysis techniques. The maximum absorbency of iron nanoparticles with the reducing ability of *P. amboinicus* leaf extract was carried out by the application of a double-beam UV-Visible spectrophotometer (UV-1990i, Shimadzu) in the wavelength range of 350–650 nm. Deionized water acted as the baseline. The crystal structure and the elemental composition within the FeONP sample were analyzed by the application of the XRD technique with Cu-Kα radiation. The scanning speed of 2°/min with a 2θ value between 20 and 80° was used. FTIR analysis was done by the application of the KBr pellet method, and identified functional groups involved in iron oxide reduction. Resolution of 4 cm^{-1} with 32 scans per sample was used. The structure of FeONPs synthesized was identified by the application of the above-mentioned characterization techniques [16].

Antimicrobial activity against pathogens

Antimicrobial activities of FeONPs synthesized using *P. amboinicus* leaf extract, FeONPs-based nanocomposites, and crude leaf extracts were tested against *S. aureus*, *S. epidermidis*, *S. mutans*, *A. actinomycetemcomitans,* and *C. albicans*. These pathogenic isolates (18 h incubation in brain heart infusion [BHI] broth) were standardized to an inoculum Concentration of 0.5 McFarland turbidity (~1 × 10^8 CFU/mL). The Mueller–Hinton agar plates were prepared. 8 mm wells were created aseptically; 25, 50, or 100 µL from each test sample was added to each well. Amoxicillin was used as the positive control for bacteria and Fluconazole for *C. albicans*. Plates were incubated at 37°C for 24 h, and the diameters of inhibition zones were measured [17]. The minimum inhibitory concentration (MIC) is a gold standard, assayed using the standard microbroth dilution method, wherein serial two-fold dilutions of the samples were prepared in BHI broth for bacteria and Sabouraud Dextrose broth for *C. albicans*, and further inoculated with standardized microbial suspensions and incubated at 37°C for 24 h; the MIC was identified as the lowest concentration presenting no visible microbial growth, using amoxicillin and fluconazole as positive controls.

Time kill curve assay

The antimicrobial activity of FeONPs synthesized using the green method with *P. amboinicus* leaf extract as the reducing and stabilizing agent in a time-dependent manner was checked using the standard time-kill curve test [18] as follows: The pathogenic isolates include *A. actinomycetemcomitans*, *S. mutans*, *S. aureus*, *S. epidermidis*, and *C. albicans*. Cultures of the bacterial isolates were maintained in BHI agar plates and incubated at 37°C. The turbidities of all bacterial cultures were adjusted to 0.5 McFarland standards (~1 × 10^8 CFU/mL). The diluted cultures were further diluted 1:100 in BHI in each sample. The bacterial concentration reached ~1 × 10^6 CFU/mL (0.5 McFarland). At 25, 50, and 100 µg/mL, the FeONP sample solutions were added. Bacterial samples without the FeONPs served as negative controls. Finally, all the samples were incubated in BHI broth at 37°C. Od 600 nm was measured using a UV-Visible spectrophotometer at defined times of 0, 1, 2, 3, 4, and 5 h. Graphs showing OD values plotted as a function of time were made.

Antioxidant assay

1 mL of 2,2-diphenyl-1-picrylhydrazyl (DPPH) was combined with 450 µL of TrisHCl buffer and FeONPs of *P. amboinicus* extract in different concentrations (10, 20, 30, 40, and 50 µg/mL) to conduct the free radical scavenging DPPH assay of *P. amboinicus* leaves extract mediated FeONPs [19]. 30 min were then spent incubating the mixture. Free radical scavenging was determined by calculating absorbance at 517 nm. Ascorbic acid was employed as the control. The equation was used to calculate the % inhibition.

$$\%of\ inhibiton = \frac{Absorbance\,of\,control - Absorbance\,of\,sample}{Absorbance\,of\,control} \times 100$$

Egg albumin (EA) denaturation assay

It consisted of 0.2 mL of 1% fresh EA and 2.8 mL of 1× phosphate-buffered saline (PBS) solution with a pH of 6.4. It was mixed with *P. amboinicus*-FeONPs at various concentrations (10, 20, 30, 40, and

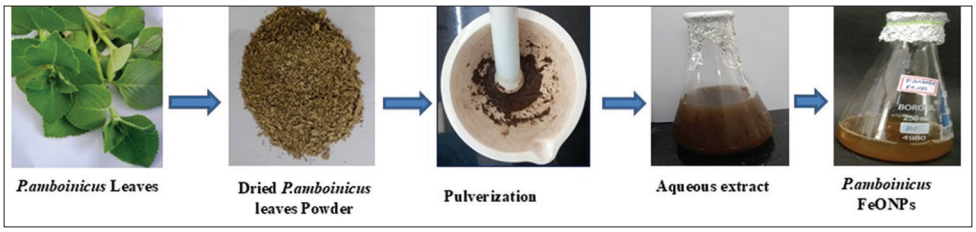

Fig. 1: Schematic of the green synthesis of iron oxide nanoparticles using *Plectranthus amboinicus* extract

50 µg/mL) in 2 mL. 2 mL of diclofenac sodium was used as the positive control. The mixtures were shaken well. After that, the mixtures were incubated for 15 min at 37°C. The mixtures were denatured for 5 min in a 70°C water bath. A UV-visible spectrophotometer analyzed the absorbance of the albumin solution at 660 nm after it had cooled down [20].

The following formula was used to determine the inhibition percentage of EA denaturation:

$$\%of\ inhibiton = \frac{Absorbance\,of\ control - Absorbance\,of\ sample}{Absorbance\,of\ control} \times 100$$

Bovine serum albumin (BSA) denaturation assay

The anti-inflammatory properties of *P. amboinicus*-induced FeONPs were assessed by BSA denaturation assay with few modifications based on their properties [21]. The process involved the use of 1 mL of 1% BSA prepared in PBS solution with pH 6.4 and various concentrations of FeONPs (10–50 µg/mL), incorporating diclofenac sodium acting as a standard drug for the study. The controls used were PBS without the sample solution to be tested. All samples were left to incubate for 20 min at 37°C and subsequently underwent heat denaturation at 70°C for 5 min in a water bath. After this process, the samples underwent cooling and subsequent measurements to detect the inhibition rate of denaturation of proteins by the spectrophotometer by observing the samples at 660 nm wavelength in UV-Vis spectrophotometer.

The following formula was used to determine the percentage inhibition of BSA denaturation because the control represents 100% protein denaturation:

$$\%of\ inhibiton = \frac{Absorbance\,of\ control - Absorbance\,of\ sample}{Absorbance\,of\ control} \times 100$$

Cytotoxicity activity

Artificial seawater solutions were made by adding 2 g of non-iodized salt to 200 mL of doubly distilled water. Ten nauplii of brine shrimp were placed into each well of a six-well plate prefilled with 10–12 mL of saline solution. The wells received FeONPs with a concentration of 5, 10, 20, 40, or 80 µg/mL, with a saline control group. The plates contained cells for 24 h of normal lighting conditions. Cell death was calculated manually with a binocular stereo microscope, separating life and death brine shrimp larvae [22]. The formula for percentage of cell death was:

$$\%lethality = \frac{Number\ of\ dead\ nauplii}{Number\ of\ dead\ nauplii + Number\ of\ live\ nauplii} \times 100$$

Statistical analysis

The data analysis was conducted using GraphPad Prism software version 10. The two-way analysis of variance (ANOVA) test accompanied by the Tukey post-test analysis was applied to compare differences in the treated and control groups. The experiment was conducted 3 times in a triplicate manner (n=3), and the data are expressed in mean standard deviation.

RESULTS

Visual observation

A color change was noticed after the reaction; the precursor mixture was dark brown in color, while the reaction product appeared light brownish-orange as can be seen in Fig. 2a and b, respectively. This indicates a successful conversion of the iron salts into FeONPs using the *P. amboinicus* extract.

Optical analysis using UV-visible spectrophotometer

The UV-Vis spectrum of the *P. amboinicus*-mediated FeONPs showed a broad peak ranging between 380 nm and 410 nm, attributed to the broad Surface Plasmon Resonance (SPR)-like absorbance properties of Fe_3O_4/Fe_2O_3 nanostructures. This is in contrast to that observed in noble metal nanostructures. The broadness of the observed peaks in the current study is in line with what had previously been observed in FeONPs, as noted in various studies [23]. The broadness of these peaks is an indication that the FeONPs had been synthesized in the laboratory.

All the replicates had a similar spectrum with hardly any variation in the intensity of the peaks, indicating that the results had a high level of accuracy and that there was not any agglutination. Furthermore, the fact that there were no other peaks within the spectrum being recorded indicated that the nanoparticles that had been synthesized had a high level of purity and that there were no phytochemicals that had not been bound or other ions of the metals (Fig. 3).

XRD analysis

The XRD pattern of P. amboinicus-mediated FeONPs showed broad diffraction peaks at 2θ values of 27.329°, 33.482°, 40.04°, 43.044°, 68.759°, and 83.266°, which correspond to the characteristic planes of iron oxide phases such as maghemite (γ-Fe_2O_3) or magnetite (Fe_3O_4), consistent with JCPDS standards. Peak width increases provide an indication of the nanocrystallinity of the particles. Calculations of crystallite size from the Scherrer equation ($D = K\lambda/\beta\cos\theta$), using the principal peak at 33.48°, showed an average crystallite size of about 10–12 nm. These results prove that phase-pure nanocrystalline FeONPs of low long-range order, typical of green-synthesized nanoparticles, had indeed been produced (Fig. 4).

FTIR analysis

The FTIR spectrum has further justified the use of the phytochemicals of *P. amboinicus* in the reduction and stabilization of FeONPs. The broad peak at 3324.7 cm^{-1} is due to the O–H bonds of hydroxyl groups, and the peaks at 1555.8 cm^{-1} and 1423.4 cm^{-1} correspond to the C=C and C–O bonds, respectively, resulting from the contributions of flavonoids and polyphenols. The absence of peaks related to impurities establishes the purity of the synthesized FeONPs (Fig. 5 and Table 1).

Antimicrobial activity

The antimicrobial potential of FeONPs mediated by *P. amboinicus* was tested against *S. aureus*, *S. epidermidis*, *S. mutans*, *C. albicans*, and *A. actinomycetemcomitans* with the following concentrations (25, 50, and 100 µg/mL), with Standard drugs Amoxicillin for the bacterial pathogens and fluconazole for *C. albicans* as positive controls. The data clearly confirmed the dose-dependent increase in the antimicrobial potential against all tested microorganisms (Fig. 6). The maximum

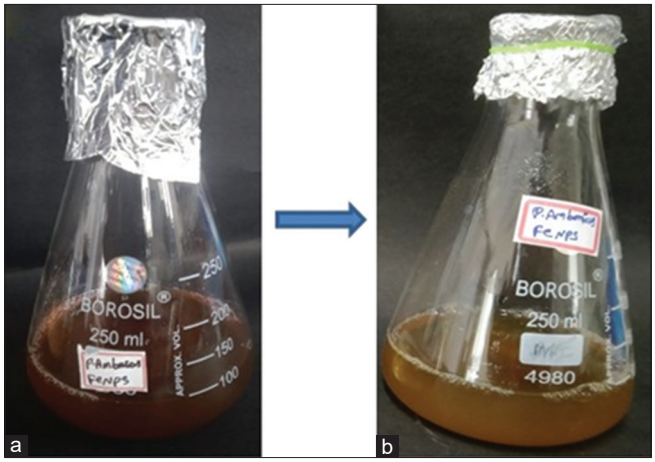

Fig. 2: Visual observation of biosynthesized iron oxide nanoparticles by *Plectranthus amboinicus* (a) Before reaction, (b) After 24 h reaction

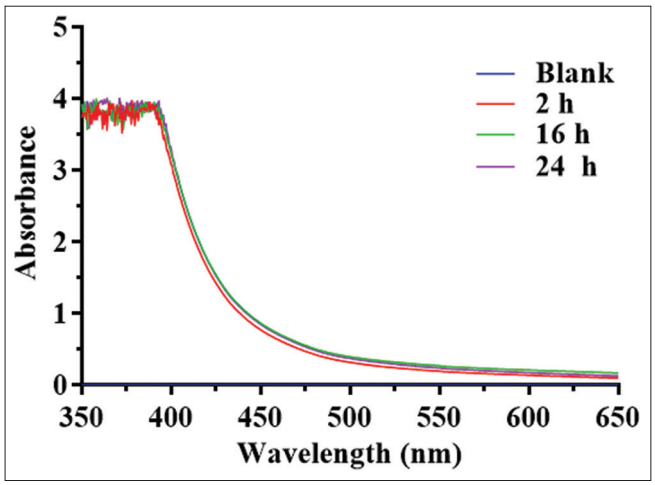

Fig. 3: Ultraviolet-visible absorption spectrum of *Plectranthus amboinicus*-mediated iron oxide nanoparticles showing a characteristic surface plasmon resonance peak at λmax = 395 nm

zones of inhibition were uniformly observed in the 100 µg/mL concentration, whereas moderate inhibitory action was observed in the 25 µg/mL concentration. The control drugs showed significantly larger zones of inhibition for all microorganisms, thus confirming the enhanced antimicrobial potential of the drugs.

The antimicrobial effect of the test samples depends significantly on the dose. The data confirmed the dose-dependent increase. On the basis of inhibition concentration-dependent data, the values of MIC were determined to evaluate quantitatively the antimicrobial action. *C. albicans* was found to be significantly more sensitive than other organisms at an inhibitor concentration of 25 µg/mL. Other organisms *S. aureus*, *S. epidermidis*, and *A. actinomycetemcomitans* were found to be moderately sensitive at an inhibitor concentration of 50 µg/mL, while *S. mutans* was found to be sensitive at an inhibitor concentration of 100 µg/mL. These observations clearly indicate the broad-spectrum antimicrobial properties of green-synthesized FeONPs.

Time kill curve assay

In the time kill experiment, there was a remarkable inhibition presented by *P. amboinicus*-mediated FeONPs against all tested bacteria and fungi, *S. aureus*, *S. epidermidis*, *S. mutans*, *C. albicans*, and *A. actinomycetemcomitans*. Although in control without treatment, the

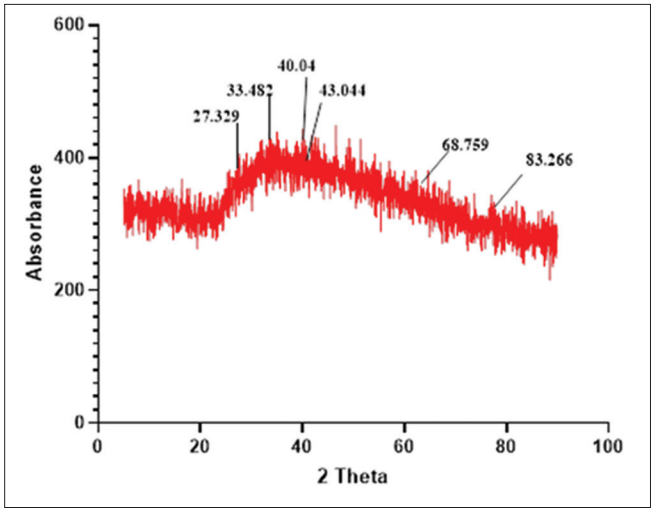

Fig. 4: X-ray diffraction pattern of *Plectranthus amboinicus*-mediated iron oxide nanoparticles. Major peaks are labeled with (hkl) indices corresponding to γ-Fe_2O_3 (JCPDS 39-1346) and Fe_3O_4 (JCPDS 19-0629)

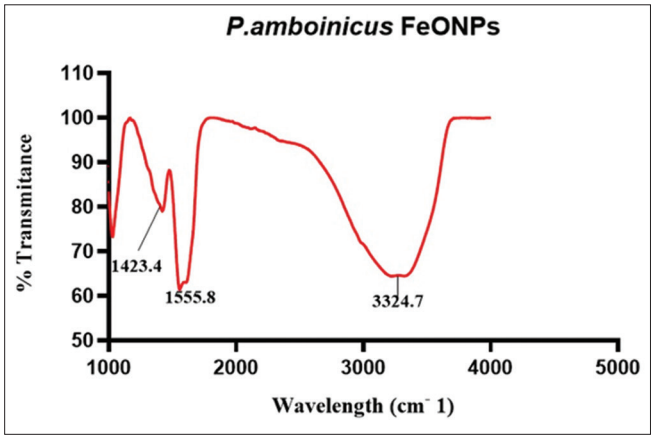

Fig. 5: Fourier transform infrared spectrum of *Plectranthus amboinicus*-mediated iron oxide nanoparticles with major peaks labeled: 3324 cm^{-1} (O–H), 1555 cm^{-1} (C=C), 1423 cm^{-1} (C–H)

Table 1: FTIR peak assignments of *Plectranthus amboinicus*-mediated FeONPs

Wavenumber (cm^{-1})	Functional group/ vibration	Probable phytochemical source
3324.7	O–H stretching (hydroxyl groups)	Phenols, flavonoids, alcohols
1555.8	C=C stretching (aromatic ring)	Flavonoids, polyphenols
1423.4	C–O stretching (alcohols/phenolics)	Polyphenols, tannins, glycosides

levels of absorption escalated and remained stable for 5 h, indicating a significant growth of microbes. In contrary, all groups treated with FeONPs concentrations of 25, 50, and 100 µg/mL indicated a drop in absorption levels with regard to the passage of time, representing an impressive inhibitory response. A drop in levels, however, represented a concentration-response approach, with 100 µg/mL consistently indicating the lowest levels of absorption every time, followed by 50 µg/mL and then 25 µg/mL. Inhibitory actions of the control drug were significantly greater than all other groups against all strains collectively. *S. mutans*, *A. actinomycetemcomitans*, and then *C. albicans*

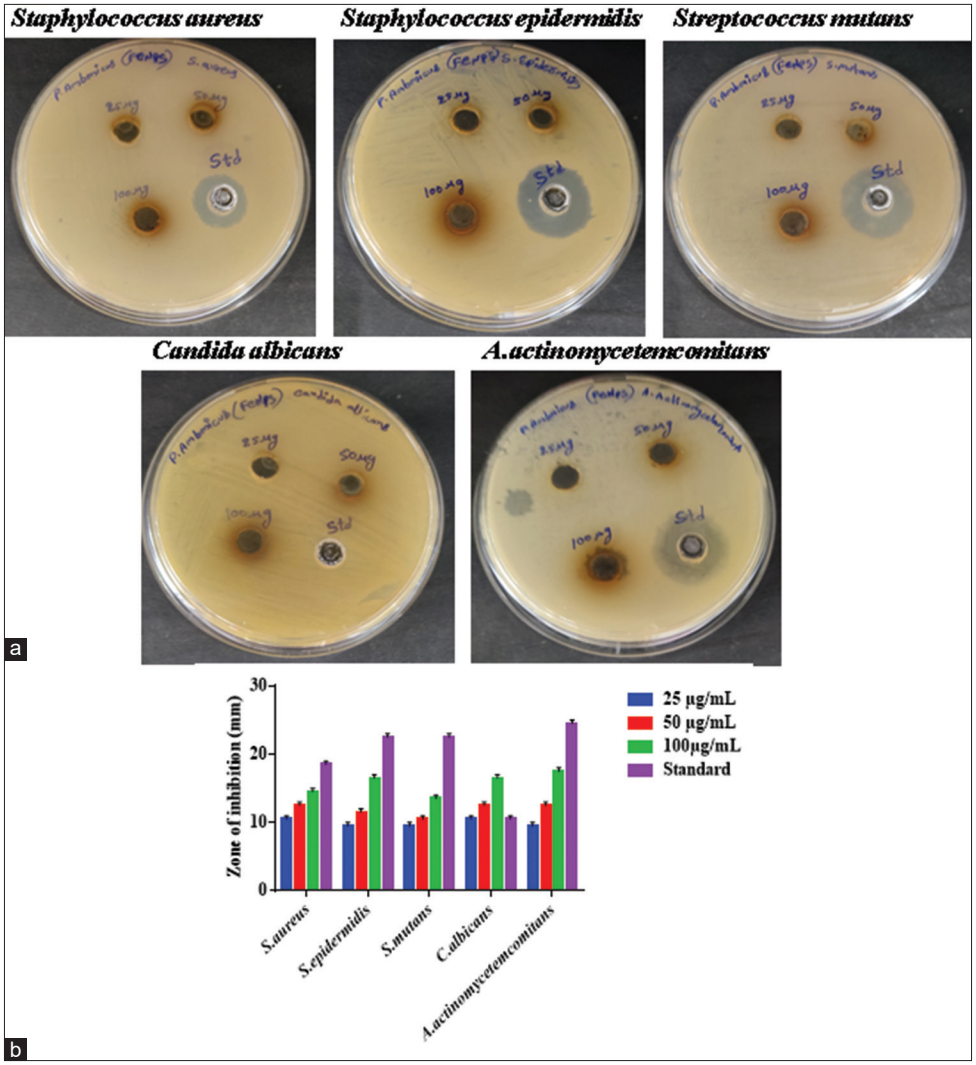

Fig. 6: Antimicrobial activity of synthesized iron oxide nanoparticles (FeONPs). (a) Agar well diffusion assay showing zone of inhibition. (b) Dose-dependent antimicrobial activity of FeONPs. Error bars represent standard deviation (n=3). Data are expressed as mean±SD (n=3). Statistical analysis was performed using two-way analysis of variance followed by Tukey's *post hoc* test. p<0.05 and p<0.01 indicate statistically significant differences between concentrations

were most sensitive to FeONPs treatment; *S. aureus* and *S. epidermidis* were less sensitive than viability (Fig. 7).

Antioxidant activities of FeONPs

Antioxidant activity of *P. amboinicus*-derived FeONPs was evaluated using the DPPH radical scavenging assay. The nanoparticles showed a clear dose-dependent inhibitory effect, with activities close to that of the reference antioxidant compound. Since the reference standard always had higher scavenging activity, statistically significant free radical neutralization by FeONPs was observed (p<0.0001). Two-way repeated measures ANOVA showed that concentration accounted for the largest proportion of variance (62.69%), followed by interaction effects (26.72%) and subject matching (8.33%), supporting the dose-dependence and reliability of FeONPs as potential antioxidants (Fig. 8).

Anti-inflammatory activities of FeONPs

Anti-inflammatory activity of FeONPs was measured by EA and BSA denaturation assays. In EA model, FeONPs showed concentration-dependent inhibition of protein denaturation, up to about 45% inhibition at 50 µg/mL, but the standard drug had more inhibition (>60%). In the BSA test, FeONPs showed almost similar activity to the standard drug at lower doses (10–20 µg/mL), but inhibition was reduced at higher doses (30–50 µg/mL). Statistical analysis attested treatment and concentration-dependent effects (p<0.0001), validating the anti-inflammatory potential of *P. amboinicus*-derived FeONPs (Fig. 9).

Cytotoxicity assessment of FeONPs

Brine shrimp lethality assay established that the FeONPs mediated by *P. amboinicus* were highly dose-dependent cytotoxic to the nauplii. The viability of the nauplii decreased progressively as the concentration of the nanoparticles increased, and the controls retained a viability of nearly 100% at all concentrations, proving the nanoparticles-specific death caused to the nauplii. The viability of the nauplii was nearly 50% for lower concentrations (5–10 µg/mL), but a significant reduction was observed for higher concentrations (40–80 µg/mL), and the viability was below 20% at a concentration of 80 µg/mL. Two-way repeated-measures ANOVA analysis depicted a highly significant effect of the treatment (p<0.0001) and a significant concentration by treatment interaction, thus proving the cytotoxic property of the nanoparticles (Figs. 10 and 11). Using the concentration-response relation, the LC_{50} value was calculated to be about 8 µg/mL, establishing the moderate cytotoxicity of the synthesized FeONPs and thereafter proving the concentration-specific biological effect of the nanoparticles, a property critical for the identification of a safe and optimal concentration of the nanoparticles.

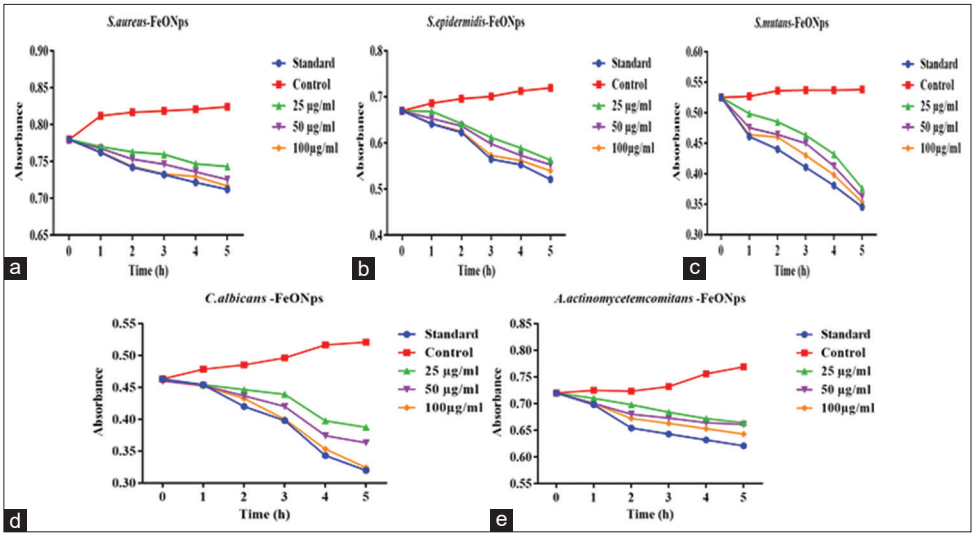

Fig. 7: Antibacterial activity of *Plectranthus amboinicus*-iron oxide nanoparticles against pathogenic bacteria (a) *Staphylococcus aureus*, (b) *Staphylococcus epidermidis*, (c) *Staphylococcus mutans*, (d) *Candida albicans*, (e) *Aggregatibacter actinomycetemcomitans.* Data are expressed as mean±SD (n=3). Statistical analysis was performed using two-way analysis of variance followed by Tukey's *post hoc* test using GraphPad Prism version 10. Differences were considered statistically significant at p<0.05 and p<0.01

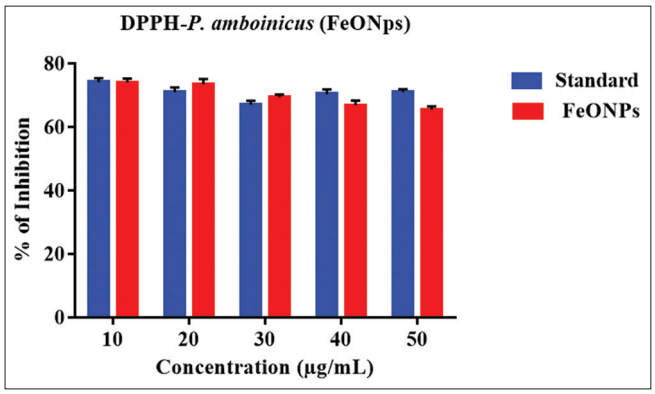

Fig. 8: Antioxidant activity of iron oxide nanoparticles compared with standard compounds (ascorbic acid for the 2,2-diphenyl-1-picrylhydrazyl assay). Data are expressed as mean±SD (n=3). Statistical analysis was performed using two-way analysis of variance followed by the appropriate Tukey's *post hoc* test. Differences were considered statistically significant at p<0.05

DISCUSSION

Visual observation

The color change is an indication of the reduction of Fe^{3+} ions and the stabilization of FeONPs by phytochemicals in the extract. The optical change is attributed to many authors as the first sign of the production of nanoparticles in green media [24]. The bioactive molecules act as reducing and capping agents, thus inhibiting agglomeration. However, further analysis was needed to confirm the size, shape, and structure of FeONPs.

UV–visible spectroscopy

The appearance of a strong absorption band corresponding to 380–410 nm is associated with SPR in FeONPs. This confirms the fact that *P. amboinicus* leaf extract acted as a strong reducing as well as stabilizing agent in the green synthesis process. The breadth of a strong absorption band points toward a uniform dispersal of nanoparticles along with regularly shaped morphology. Small differences in the measured intensity of absorption may be ascribed to differences in nanoparticle concentrations or slightly different size distributions. The fact that identical spectra have been obtained in replicates confirms the validity and uniformity of the green synthesis method. The lack of any additional peaks also confirms a high level of purity of the synthesized nanoparticles. The biocompatibility of these nanoparticles becomes essential in biomedical applications [25].

XRD analysis

The wide diffraction peaks in the XRD pattern evidently confirm the nanocrystalline nature of *P. amboinicus*-mediated FeONPs, as wider peaks are inversely proportional to the size of crystallites. The calculated size of crystallites being around 10–12 nm matches well with earlier studies revealing that plant-mediated phytochemicals are very efficient reducing and capping agents, thus hindering crystal growth and maintaining ultra-small sizes for nanoparticles. The diffused and noisy pattern of the diffractogram accurately interprets the characteristics of biologically synthesized FeONPs, in which organic materials of plant extracts are strongly entrapped at the external surfaces of nanoparticles, thus creating an apparently amorphous nature. In spite of its lower crystallinity, the appearance of Bragg peaks corresponding either to γ-Fe_2O_3 or Fe_3O_4 demonstrates well the successful synthesization of iron oxide crystals. It has already been realized that bio-capped nanocrystalline FeONPs display improved properties for catalysis, antimicrobial action, and biomedical applications owing to their high surface areas, high stability, and biologically compatible surfaces, thus proving the relevance of synthesized FeONPs for future biomedical applications [26].

FTIR analysis

FTIR analysis established that phytochemicals from *P. amboinicus* extract are reducing and capping agents used in nanoparticle synthesis. The intense O–H stretching peak at 3324.7 cm^{-1} signified hydroxyl groups from phenolic compounds, while peaks at 1555.8 cm^{-1} and 1423.4 cm^{-1} established flavonoids and polyphenols responsible for reduction and stabilization. These functional groups not only stabilize the nanoparticles by avoiding agglomeration but also endow biofunctionalization, enhancing dispersion, biocompatibility, and therapeutic efficacy [27]. Lack of impurity peaks ensures the green and effective synthesis method, and these FeONPs are extremely well-suited for biomedical and catalytic applications.

Antimicrobial activity

The concentration-dependent broad-spectrum antimicrobial potential of the MIC values supported by the antimicrobial properties of *P. amboinicus*-mediated FeONPs supplies quantitative information

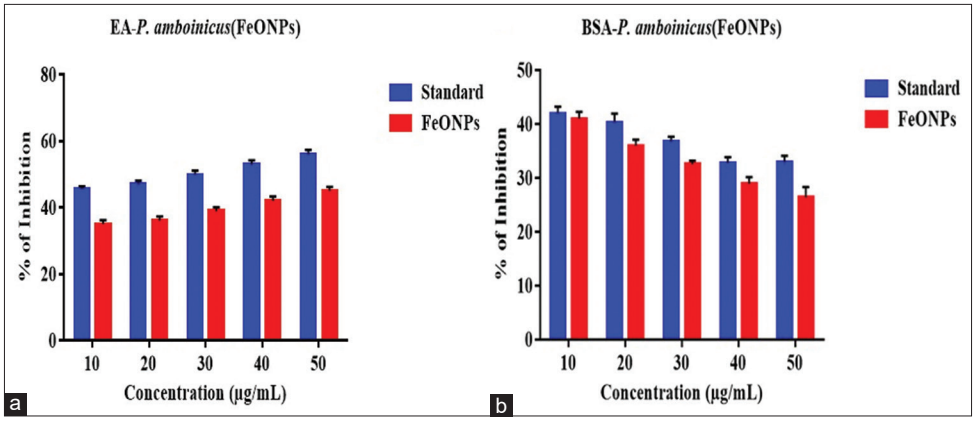

Fig. 9: (a and b) Anti-inflammatory activities of iron oxide nanoparticles compared with the standard compounds (diclofenac sodium for protein denaturation assay). Data are expressed as mean±SD (n=3). Statistical analysis was performed using one-way analysis of variance followed by an appropriate Tukey's *post hoc* test. Differences were considered statistically significant at p<0.05

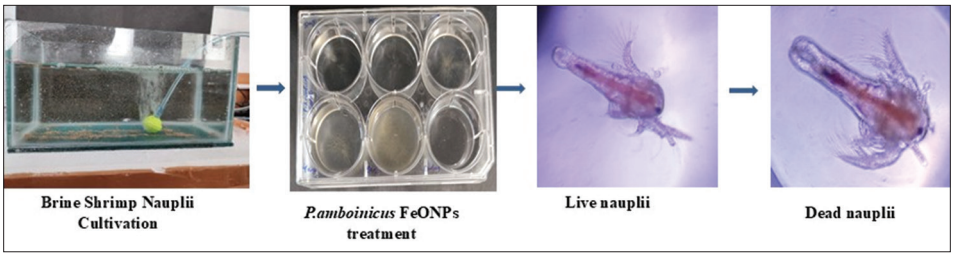

Fig. 10: Potential cytotoxic effects of iron oxide nanoparticles

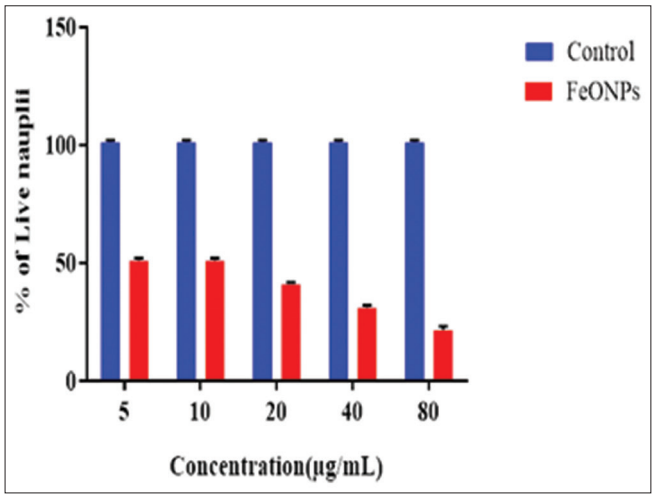

Fig. 11: Brine shrimp cytotoxicity of iron oxide nanoparticles (FeONPs). Data are expressed as mean±SD (n=3). The median lethal concentration (LC_{50}) of FeONPs was 8 µg/mL. Statistical analysis was performed using two-way analysis of variance followed by an appropriate Tukey's *post hoc* test. Differences were considered statistically significant at p<0.05

on the antimicrobial effectiveness and the susceptibility specificity of microorganisms. The relatively lower MIC required by *C. albicans* (25 µg/mL) implied greater susceptibility, and it clearly proves that FeONPs effectively interact with fungal cell wall integrity and biomolecules. However, the moderate susceptibility shown by *S. aureus* and *S. epidermidis* (MIC = 50 µg/mL) could be due to the thicker peptidoglycan layers present in their cell walls, which work as a physical barrier defending the entry and intracellular interaction of FeONPs, which has been previously discussed [28]. The relatively higher susceptibility (MIC = 100 µg/mL) among *S. mutans* could be due to its dense cell wall and stress-resistant properties, whereas the moderate susceptibility (MIC = 50 µg/mL) among *A. actinomycetemcomitans* suggested maximum intracellular interaction efficiency even though they show pathogenic properties.

The antimicrobial property of FeONPs is mainly linked with reactive oxygen species generation and membrane interaction, which are both improved at concentrations around or above the MIC values. As redox-active materials, FeONPs in microbial membranes cause the generation of oxidative stress, lipid peroxidation, protein oxidation, and finally, DNA damage due to the formation of OH and oxidative anions using their surface-active sites on microbial membranes [29]. Moreover, physical interaction between FeONPs and microbial membranes could also enhance this permeability, causing cell content leakage and failure in necessary metabolic processes. However, with their nanosized nature and high surface-to-volume ratio, FeONPs synthesized in this study further enhanced these mechanisms, which therefore justified dose-related and MIC values on these antimicrobial activities. Based on these observations, there is a promising role for using FeONPs synthesized via *P. amboinicus* as novel antimicrobial agents or as potentiating agents in combination with presently used antibacterial agents for overcoming microbial resistance.

Time-kill assay

The time-kill kinetics results provided conclusive evidence that *P. amboinicus*-synthesized FeONPs possess a strong dose-dependent inhibitory effect on microbes and fungi, with a maximum inhibitory concentration at 100 µg/mL. The drastic reduction in the number of viable cells in the *C. albicans* and *A. actinomycetemcomitans* cultures points to a significant inhibitory effect of FeONPs on microbes; thereby, FeONPs can prove to be one of the potent tools in combating fungal and periodontal infections. The low rates of microbial killing in the case of *S. aureus* and *S. epidermidis* may be attributed to their strong and multilayered peptidoglycans in the cell walls, preventing the entry of nanoparticles toward their intracellular targets.

Contrary to typical antimicrobial mechanisms, it was hypothesized that FeONPs trigger a progressive stress to cells beyond what microbes can counteract. The redox reaction of iron ions influenced cellular redox state through the inactivation of cellular enzymes, which simultaneously disrupts cellular metabolism. Simultaneously, high adhesion of the nanoparticle influenced the cellular membrane through the creation of an imbalance of ions, simultaneously leading to a time-dependent release of cytoplasm of cells. The progressive killing exhibited by the time-kill graph suggests a potential application of FeONPs either as an adjuvant agent or an alternative agent in the treatment of infections, such as biofilms, which show no response to existing antimicrobial agents currently employed in the management of infections [30].

Antioxidant assays of FeONPs

FeONPs derived from *P. amboinicus* displayed strong and concentration-dependent antioxidant activity in the DPPH radical scavenging assay [31]. The antioxidant property of FeONPs is directly related to the presence of phenolic and flavonoids in plants, which are retained on the FeONPs surface, as confirmed by FTIR analysis. The phenolic moiety of the plants has hydroxyl groups, which donate a hydrogen atom/electron, hence neutralizing DPPH free radicals [32]. Although the efficiency of FeONPs was low compared to the standard antioxidant, the findings of this research confirm that phytochemicals with redox properties are retained even after the encapsulation of plants into FeONPs. The phytochemical modification of FeONPs not only prevents their stability but also improves their antioxidant property, which facilitates electron transfer to interact with radicals. The antioxidant property of FeONPs, therefore, is mainly contributed by the phytochemical modification of *P. amboinicus* phenolic compounds, which is exclusively different from the property of iron (Fe).

Anti-inflammatory assays of FeONPs

The results indicated that *P. amboinicus*-mediated FeONPs had effective inhibition of protein denaturation, thereby expressing remarkable anti-inflammatory potential. Reduced activity at higher concentration for the BSA denaturation assay can be perceived as being due to the extra quantity of nanoparticle-protein interaction, inducing conformational stress or partial destabilization of protein rather than stabilization [33]. Optimal dosing permits protection of protein structure by hydrogen bonding and electrostatic interaction between phytochemicals surface-bound on FeONPs, while higher dosing may induce aggregation effects that reduce the protective efficacy. This biphasic dose-dependent behavior indicates that optimization of concentration is considerable for achieving high anti-inflammatory performance [34].

Brine shrimp toxicity

The brine shrimp lethality bioassay resulted in concrete evidence regarding the dose-dependent cytotoxicity of *P. amboinicus*-mediated FeONPs, in which toxic effects significantly increased as the concentration level increased with an estimated LC_{50} value of about 8 µg/mL. However, the rapid reduction in the number of alive nauplii in the high concentration values (approximately above 40 µg/mL) indicated possible toxic effects caused by excessive accumulation of nanoparticles at the cellular level as a consequence of redox imbalances resulting in oxidative damage and subsequent cell death. Although the cytotoxic effects caused by these nanoparticles restrict their non-toxic use as FeONPs at high concentrations, the effects also mark their importance in terms of their utility as therapeutic reagents in antimicrobial and antitumor applications in which their cytotoxic properties become highly beneficial as an adjunct therapy in certain situations [35]. Moreover, the less toxic effects caused by sub-LC_{50} values also indicated the existence of a therapeutic window in FeONPs in which these nanoparticles can provide biological effects without being detrimental to biocompatibility. In any situation, these outcomes highlighted the need for precise use of nanoparticles based on their concentration effects without restricting their utility in forthcoming *in vivo* studies as preliminary investigations in the use of bioassays in estimating toxic effects caused by nanoparticles [36].

CONCLUSION

The present study successfully establishes the green and eco-friendly procedure for the biogenic synthesis of FeONPs, using the leaf extract of *P. amboinicus*. The biogenically prepared FeONPs were nanocrystalline, phase-pure, having a diameter of 10–12 nm with assured surface biofunctionalization through phytochemicals such as phenolic and flavonoids. Biogenic FeONPs exhibited a broad-spectrum and concentration-dependent antibacterial and antifungal activities, notably against oral and periodontal pathogens *S. mutans* and *A. actinomycetemcomitans*. High antioxidant activity in DPPH assays and potent anti-inflammatory properties by protein-denaturation inhibition were also confirmed. Cytotoxicity tests using the brine shrimp lethality bioassay proved the moderate, concentration-dependent toxicity with an approximate LC_{50} of 8 µg/mL, hence establishing a safe therapeutic index for biomedical formulation and application. The results also tend to point out the anticancer activity that requires further research work using suitable cancer cells.

P. amboinicus-mediated FeONPs have huge potential as a multi-functional nanomaterial for antimicrobial, antioxidant, anti-inflammatory, and anticancer therapies. For future research, the validation studies are to be emphasized with appropriate animal models to analyze the pharmacokinetics and biological distribution of these particles. Studies at the molecular and cellular levels and research involving cancer cell cultures are integral to comprehending the exact mechanism by which these particles exert their actions as antimicrobials, antioxidants, anti-inflammatory, and anticancer. Besides, functionalizing these particles through conjugation to targeting ligands can help in achieving specificity and activity that may further help formulate a target drug delivery system. In fact, all these upcoming research endeavors are going to bring about a revolutionary change to translate these particles, extracted from *P. amboinicus*, as safe and effective nanotherapeutic agents.

ACKNOWLEDGEMENT

My profound gratitude is extended to my mentor, Dr. S. Sivamalar, for her support and direction, as well as to the faculty of the Meenakshi Academy of Higher Education and Research's Department of Research for their assistance and direction.

AUTHORS CONTRIBUTIONS

SS performed the assessment. YS wrote the initial draft. SS reviewed the manuscript, edited, and approved the final manuscript for publication.

CONFLICT OF INTEREST

The authors declare that there is no conflict of interest**.**

FUNDING

No funding has been obtained.

REFERENCES

1. Khan I, Saeed K, Khan I. Nanoparticles: Properties, applications and toxicities. Arab J Chem. 2019 Nov;12(7):908-31. doi: 10.1016/j.arabjc.2017.05.011
2. Alvi GB, Iqbal MS, Ghaith MM, Haseeb A, Ahmed B, Qadir MI. Biogenic selenium nanoparticles (SeNPs) from citrus fruit has anti-bacterial activities. Sci Rep. 2021;11:4811. doi: 10.1038/s41598-021-84330-w
3. Koul B, Poonia AK, Yadav D, Jin JO. Microbe-mediated biosynthesis of nanoparticles: Applications and future prospects. Biomolecules. 2021 Jun 15;11(6):886. doi: 10.3390/biom11060886, PMID 34203733, PMCID PMC8246319
4. Sathiyavimal S, Vasantharaj S, Veeramani V, Saravanan M, Rajalakshmi G, Kaliannan T, *et al*. Green chemistry route of biosynthesized copper oxide nanoparticles using *Psidium guajava* leaf extract and their antibacterial activity and effective removal of industrial dyes. J Environ Chem Eng. 2021 Apr 1;9(2):105033.

doi: 10.1016/j.jece.2021.105033
5. Vasantharaj S, Sathiyavimal S, Senthilkumar P, LewisOscar F, Pugazhendhi A. Biosynthesis of iron oxide nanoparticles using leaf extract of *Ruellia tuberosa*: Antimicrobial properties and their applications in photocatalytic degradation. J Photochem Photobiol B. 2019 Mar 1;192:74-82. doi: 10.1016/j.jphotobiol.2018.12.025, PMID 30685586
6. Yadi M, Mostafavi E, Saleh B, Davaran S, Aliyeva I, Khalilov R. Current developments in green synthesis of metallic nanoparticles using plant extracts: A review. Green Chem Lett Rev. 2018;11(4 sup3): 336-43. doi: 10.1080/21691401.2018.1492931.
7. Nagime PV, Chandak VS. A comprehensive review of nanomaterials synthesis: Physical, chemical, and biological approaches and emerging challenges. Biocatal Agric Biotechnol. 2024 Dec;62:103458. doi: 10.1016/j.bcab.2024.103458
8. Edo GI, Mafe AN, Ali AB, Akpoghelie PO, Yousif E, Isoje EF, *et al*. Green biosynthesis of nanoparticles using plant extracts: Mechanisms, advances, challenges, and applications. BioNanoScience. 2025 Jun;15(2):267. doi: 10.1007/s12668-025-01883-w
9. Salayová A, Bedlovičová Z, Daneu N, Baláž M, Lukáčová Bujňáková Z, Balážová Ľ *et al*. Green synthesis of silver nanoparticles with antibacterial activity using various medicinal plant extracts: Morphology and antibacterial efficacy. Nanomaterials (Basel). 2021 Apr 14;11(4):1005. doi: 10.3390/nano11041005, PMID 33919801
10. Jayaweera JM, Ravihari AK, Kuruppu KA, Perera KI, Lathurshan K, Dunukara JD, *et al*. Antimicrobial activity of *Plectranthus amboinicus*, *Bacopa monnieri*, *Flueggea leucopyrus* and *Cymbopogon citratus* plant extracts against common pathogens. Sri Lankan J Infect Dis. 2023;13 Suppl 5:PP17-A8. doi: 10.4038/sljid.v13i5.8651
11. de Mendonça LG, Zambelli RA. Health-promoting properties of *Plectranthus amboinicus*: A comprehensive review. J Nutr Health. 2023;1(1):17-21. doi: 10.61577/jnh.2023.100004
12. Caroline ML, Muthukumar RS, Harini Priya AH, Nachiammai N. Anticancer effect of *Plectranthus amboinicus* and *Glycyrrhiza glabra* on oral cancer cell line: An *in vitro* experimental study. Asian Pac J Cancer Prev. 2023 Mar 1;24(3):881-7. doi: 10.31557/APJCP.2023
13. Mehmood A, Murtaza G, Bhatti TM, Kausar R. Phyto-mediated synthesis of silver nanoparticles from *Melia azedarach* leaf extract: Characterization and antibacterial activity. Arab J Chem. 2017;10:S3048-53. doi: 10.1016/j.arabjc.2013.11.046
14. Abbasi BA, Iqbal J, Zahra SA, Shahbaz A, Kanwal S, Rabbani A, *et al*. Bioinspired synthesis and activity characterization of iron oxide nanoparticles made using *Rhamnus triquetra* leaf extract. Mater Res Express. 2020;6(12):1250e7. doi: 10.1088/2053-1591/ab664d
15. Bharathi D, Ranjithkumar R, Vasantharaj S, Chandarshekar B, Bhuvaneshwari V. Synthesis and characterization of chitosan/iron oxide nanocomposite for biomedical applications. Int J Biol Macromol. 2019 Jul 1;132:880-7. doi: 10.1016/j.ijbiomac.2019.03.233, PMID 30940585
16. Abid MA, Abid DA, Aziz WJ, Rashid TM. Iron oxide nanoparticles synthesized using garlic and onion peel extracts rapidly degrade methylene blue dye. Phys B Condens Matter. 2021 Dec 1;622:413277. doi: 10.1016/j.physb.2021.413277
17. Hayat P, Khan I, Rehman A, Jamil T, Hayat A, Rehman MU, *et al*. Myogenesis and analysis of antimicrobial potential of silver nanoparticles (AgNPs) against pathogenic bacteria. Molecules. 2023;28(2):637. doi: 10.3390/molecules28020637, PMID 36677695
18. Shah SS, Turakhia BP, Purohit N, Kapadiya KM, Sahoo CR, Prajapati A. Facile green synthesis of iron oxide nanoparticles and their impact on cytotoxicity, antioxidative properties and bactericidal activity. Iran Biomed J. 2024 Mar 1;28(2&3):71-81. doi: 10.61186/ibj.4061, PMID 38770844
19. Foerster S, Unemo M, Hathaway LJ, Low N, Althaus CL. Time-kill curve analysis and pharmacodynamic modelling for in vitro evaluation of antimicrobials against *Neisseria gonorrhoeae*. BMC Microbiol. 2016 Dec;16:216. doi: 10.1186/s12866-016-0838-9, PMID 27639378
20. Bailey-Shaw YA, Williams LA, Green CE, Rodney S, Smith AM. *In-vitro* evaluation of the anti-inflammatory potential of selected Jamaican plant extracts using the bovine serum albumin protein denaturation assay. Int J Pharm Sci Rev Res. 2017 Nov-Dec;47(1):145-53.
21. Gunathilake KD, Ranaweera KK, Rupasinghe HP. *In vitro* anti-inflammatory properties of selected green leafy vegetables. Biomedicines. 2018 Nov 19;6(4):107. doi: 10.3390/biomedicines6040107, PMID 30463216
22. Banti CN, Hadjikakou SK. Evaluation of toxicity with brine shrimp assay. Bio Protoc. 2021 Jan 20;11(2):e3895. doi: 10.21769/BioProtoc.3895, PMID 33732784
23. Fahmy HM, Mohamed FM, Marzouq MH, Mustafa AB, Alsoudi AM, Ali OA, *et al*. Review of green methods of iron nanoparticles synthesis and applications. BioNanoScience. 2018;8(2):491-503. doi: 10.1007/s12668-018-0516-5
24. Manimaran K, Yanto DH, Govindasamy M, Karunanithi B, Alasmary FA, Habab RA. Biological synthesis and characterization of iron oxide (FeO) nanoparticles using *Pleurotus citrinopileatus* extract and its biomedical applications. Biomass Convers Biorefin. 2024 Jun;14(11):12575-85. doi: 10.1007/s13399-023-04382-8
25. Grasso G, Zane D, Dragone R. Microbial nanotechnology: Challenges and prospects for green biocatalytic synthesis of nanoscale materials for sensoristic and biomedical applications. Nanomaterials (Basel). 2019;10(1):11. doi: 10.3390/nano10010011, PMID 31861471
26. Xu C, Akakuru OU, Zheng J, Wu A. Applications of iron oxide-based magnetic nanoparticles in the diagnosis and treatment of bacterial infections. Front Bioeng Biotechnol. 2019;7:141. doi: 10.3389/fbioe.2019.00141, PMID 31275930
27. Monica K, Rajeshkumar S, Ramasubramanian A, Ramani P, Sukumaran G. Anti-inflammatory and antimicrobial effects of herbal formulation using karpooravalli, mint, and cinnamon on wound pathogens. J Adv Pharm Technol Res. 2022 Dec;13 Suppl 2:S369-73. doi: 10.4103/japtr.japtr_515_22, PMID 36798541
28. Mohamad EA, Ramadan MA, Mostafa MM, Elneklawi MS. Enhancing the antibacterial effect of iron oxide and silver nanoparticles by extremely low frequency electric fields (ELF-EF) against *S. aureus*. Electromagn Biol Med. 2023 Jul 3;42(3):99-113. doi: 10.1080/15368378.2023.2208610, PMID 37154170
29. Shreya S, Suma BV. Synthesis and evaluation of a coumarin Schiff-base for *in vitro* antibacterial activity against *Staphylococcus aureus*. Int J Pharm Pharm Sci. 2024;16(12):26-30. doi: 10.22159/ijpps.2024v16i12.52430
30. Naveed M, Batool H, Rehman SU, Javed A, Makhdoom SI, Aziz T, *et al*. Characterization and evaluation of the antioxidant, antidiabetic, anti-inflammatory, and cytotoxic activities of silver nanoparticles synthesized using *Brachychiton populneus* leaf extract. Processes. 2022;10(8):1521. doi: 10.3390/pr10081521
31. Elya B, Nur S, Iswandana R. Formulation, antioxidant, and anti-aging activity of *Rubus fraxinifolius* fraction. Int J Appl Pharm. 2024;16(4):121-8.
32. Sulistyowati, Elya B, Nur S, Iswandana R. Formulation, antioxidant, and anti-aging activity of *Rubus Fraxinifolius* fraction. Int J Appl Pharm. 2024;16(4):121-8. doi: 10.22159/ijap.2024v16i4.51013
33. Jaswal S, Sidana A, Mehta S, Gupta S, Kaur G. The clinical observation of inflammation theory for schizophrenia: A 12 week interventional study. Int J Curr Res. 2025;17(11):35207-13. doi: 10.24941/ijcr.49746.11.2025
34. Minhas LA, Kaleem M, Minhas MA, Waqar R, Al Farraj DA, Alsaigh MA, *et al*. Biogenic fabrication of iron oxide nanoparticles from *Leptolyngbya* sp. L-2 and multiple *in vitro* pharmacogenetic properties. Toxics. 2023 Jun 27;11(7):561. doi: 10.3390/toxics11070561, PMID 37505527
35. Wakawa HY, Fasihuddin BA. Brine shrimp lethality bioassay of *Abrus precatorius* (Linn) leaves and root extract. Int J Pharm Pharm Sci. 2016;9(1):179-81. doi: 10.22159/ijpps.2017v9i1.15057
36. Ashraf N, Ahmad F, Da-Wei L, Zhou RB, Feng-Li H, Yin DC. Iron/iron oxide nanoparticles: Advances in microbial fabrication, mechanism study, biomedical, and environmental applications. Crit Rev Microbiol. 2019;45(3):278-300. doi: 10.1080/1040841X.2019.1593101, PMID 30985230